

## Traveling wave-induced aerodynamic propulsive forces using piezoelectrically deformed substrates

Noah T. Jafferis,<sup>1,2,a)</sup> Howard A. Stone,<sup>2,3</sup> and James C. Sturm<sup>1,2</sup>

<sup>1</sup>*Department of Electrical Engineering, Princeton University, Princeton, New Jersey 08544, USA*

<sup>2</sup>*Princeton Institute for the Science and Technology of Materials (PRISM), Princeton University, Princeton, New Jersey 08544, USA*

<sup>3</sup>*Department of Mechanical and Aerospace Engineering, Princeton University, Princeton, New Jersey 08544, USA*

(Received 1 July 2011; accepted 22 August 2011; published online 13 September 2011)

We use integrated piezoelectric actuators and sensors to demonstrate the propulsive force produced by controllable transverse traveling waves in a thin plastic sheet suspended in air above a flat surface, thus confirming the physical basis for a “flying” carpet near a horizontal surface. Experiments are conducted to determine the dependence of the force on the height above the ground and the amplitude of the traveling wave, which qualitatively confirm previous theoretical predictions. © 2011 American Institute of Physics. [doi:10.1063/1.3637635]

A thin sheet deformed as a function of time in a traveling wave shape has been predicted to produce a force in the direction opposite that of the wave propagation.<sup>1,2</sup> The resulting forward motion of the sheet near the ground has been predicted to produce a lift force,<sup>3</sup> leading to a so-called “flying” carpet.<sup>4</sup> This letter describes the experimental demonstration that a thin sheet, deformed in a traveling wave shape by integrated piezoelectric actuators, generates a propulsive force that propels the sheet forward in air.

To gain a basic understanding of why a traveling wave shape will propel the sheet, imagine that the sheet begins at a height  $h_0$  above the ground, is stationary, and has no tilt. When the sheet begins to bend in the shape of a traveling wave, a pocket of the surrounding fluid (air in our case) is pulled in from the front end and is carried along with the wave until it reaches the back end of the sheet, where it is released (Fig. 1). Thus, the traveling wave acts as a pump (such pumping has been demonstrated in glycerol and water<sup>5</sup>). Since the wave acts to push fluid in the direction of the wave, there must be a corresponding force that the fluid exerts on the sheet in the direction opposite to the wave. If  $h_0$  is comparable to or larger than the lateral dimensions of the sheet, the pump will have significant leakage, since the fluid is free to move perpendicularly away from the sheet as well. When  $h_0$  is reduced, the confined space significantly reduces this leakage on the side of the sheet that faces the ground, and consequently, the propulsive force should increase as the gap between the sheet and the ground is diminished.

In our experiments, two sheets of metal-coated polyvinylidene fluoride (PVDF; thickness of each sheet is  $t_{PVDF} = 28 \mu\text{m}$ , Young’s Modulus is  $\sim 2 \text{ GPa}$ , and piezoelectric coefficients are  $d_{31} = 23 \text{ pC/N}$  and  $d_{32} = 2.3 \text{ pC/N}$ ) are glued together with a thin epoxy layer ( $t_{Epoxy} \approx 30 \mu\text{m}$ ). The metal coating on both sides of each PVDF sheet is patterned into eight regions—four of which are used as actuators (25 mm by 35 mm) and four of which are used as sensors (25 mm by 3 mm) (Fig. 2).

<sup>a)</sup> Author to whom correspondence should be addressed. Electronic mail: jafferis@princeton.edu.

Loose conducting threads (diameter  $\sim 50 \mu\text{m}$ ) are attached to each electrode and to the common plane between the sheets to apply and sense voltages. Time-varying voltages are applied to each actuator region on the two PVDF sheets, with opposite polarity in each sheet (relative to the polarization direction). This causes one sheet to locally expand in the plane of the sheet, and the other to contract, causing a local curvature. The sensors are used to measure the actual time-varying shape of the sheet, which allows the actuator control signals to be adjusted to produce a traveling wave. This step is necessary because at higher frequencies ( $> 10 \text{ Hz}$ ) dynamic effects and nonlinearities would cause the deformations to be far from a traveling wave. We measure the linear control matrix that relates the four applied voltages to the four measured curvatures, and by applying feedback separately for each harmonic with a “significant” undesired component present, we are able to cancel out all but the desired fundamental frequency of the traveling wave. Figure 3 shows an example of these measurements and demonstrates the need for integrated sensors and feedback. Figures 3(a) and 3(b) show, respectively, the applied voltages and measured curvatures without using the sensors. The applied voltages are then adjusted using the sensors and feedback (Fig. 3(c)), and the resulting curvatures (Fig. 3(d)) indicate a traveling wave deformation. The applied voltages were chosen to create a deformation with a wavelength equal to that of the sheet (10 cm). A high-speed camera confirmed that the deformation of the sheet, inferred from the sensor measurements of curvature, was indeed a traveling wave, with wave amplitude agreeing to within  $\sim 30\%$ .

Two experimental arrangements are used to support the sheet, both of which allowed us to measure the force produced by the traveling wave. The sheet is not entirely free, since external connections are required for power and control circuitry. In one arrangement, the sheet is suspended from three 1 m-long threads (distinct from the conductive threads mentioned above), which are elastic to allow the sheet the freedom to bend as desired. Fortunately, this setup is effectively a simple pendulum, in which the restoring force  $F_r$  due to gravity when the

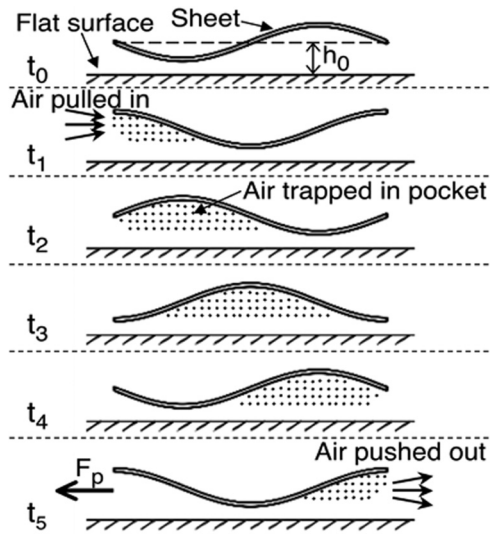


FIG. 1. Traveling-wave pump. The shape of the sheet is shown at a sequence of times ( $t_0$ – $t_5$ ) over one and a half periods of oscillation. This time-varying shape pulls air in from the left, and pushes it out to the right, resulting in a propulsive force,  $F_p$ , to the left.

sheet is displaced horizontally by a distance  $\Delta x$  is given by  $F_r \approx mg\Delta x/D$ , where  $D$  is the length of the pendulum. Thus, measurement of the displacement allows calculation of the propulsive force. To ensure that the sheet is balanced at all times, three elastic threads are needed, one at each end and one in the center with twice the spring constant (this is achieved by using two threads in the center). To see why, first note that to prevent the sheet from tipping, any forces from suspension threads must be symmetrical about the center at all times. For a traveling wave shape, this means that any supports not at the center must be one wavelength apart, i.e., at the two ends of the sheet in our case. In addition, the average height of the sheet must be fixed in time, so a thread of twice the spring constant is needed in the center of the sheet to compensate for the ones at the ends (the center thread supports twice the mass as the end threads).

In the second arrangement, the sheet is elevated above a miniature “air table,” so no threads are needed for suspension.

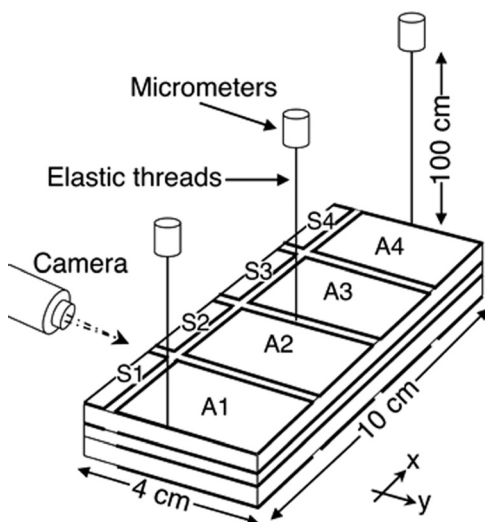


FIG. 2. Model of the experimental arrangement, showing PVDF bilayer with electrodes, suspension from elastic threads, and microscope for imaging. The metal layers are patterned to form actuators (A1–A4) and sensors (S1–S4), and electrical connections are made using conductive threads.

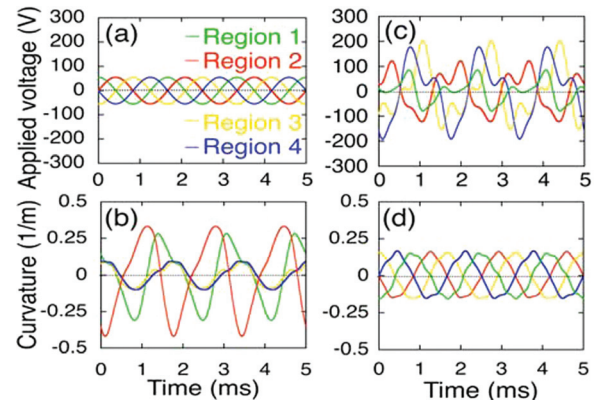


FIG. 3. (Color) Demonstration of a traveling wave, showing the significance of sensors and feedback for achieving an ideal traveling wave shape. Data shown are at 600 Hz. The upper axis (a) and (c) shows the applied voltages to the 4 pairs of actuators, and the lower axis (b) and (d) shows the average curvatures as determined from the sensor readouts. (a) and (b) Without using sensors, the shape is close to a standing wave rather than a traveling wave. (c) and (d) Feedback on higher order modes up to 5 times the fundamental is needed to achieve a traveling wave shape.

The force required to move the sheet laterally a given distance is measured directly using a force sensor (an approximately linear restoring force exists due to a combination of the electrical connections and the airflow of the air table). The force sensor, a thin plastic “whisker,” was calibrated by using weights to measure the force required to deflect the whisker by a given amount. This experimental arrangement is “cleaner” but makes it more difficult to adjust the height between the sheet and the table. The restoring force constant  $k$  is  $\sim 6 \mu\text{N}/\text{mm}$  and  $\sim 11 \mu\text{N}/\text{mm}$  in the hanging and air table configurations, respectively.

When an optimized travelling wave at 100 Hz and amplitude  $\sim 400 \mu\text{m}$  was induced in the sheet in either arrangement, the sheet moved in the direction opposite to that of the travelling wave, as expected from Fig. 1, and then reached a steady-state displacement due to the restoring force (Fig 4(a)). The direction of the displacement reversed when the wave direction was reversed. The displacement increased for smaller  $h_0$ , presumably because of less “leaky” air pumping. Typical displacements and average velocities of the sheet were  $\sim 5 \text{ mm}$  and  $\sim 10 \text{ mm/s}$ , respectively.

The theory of Ref. 4 assumes an ideal unconstrained sheet and predicts a steady-state velocity as an output, not a propulsive force. We can compare our displacement results to this theory by relating our observed displacements to a propulsive force and by determining what propulsive force is needed to propel a sheet forward at a given velocity in steady state. Since we know the restoring force constant in our experiment, from the observed displacement of the sheet, we can easily determine the propulsive force induced by the traveling wave. To determine the theoretical propulsive force, we first note that for a flat sheet moving freely close to a boundary, under low Reynolds number conditions, the drag force is given by:  $F_{\text{drag}} = v\mu_{\text{air}}WL/h$ , where  $v$  is the velocity of the sheet,  $W$  and  $L$  are its width and length,  $h$  is the height above the ground, and  $\mu_{\text{air}}$  is the air viscosity. For a sheet moving freely and in equilibrium, the air flow pushed backwards by the traveling wave must equal the air flow pushed forward by the sheet’s forward motion:  $Af\lambda \sim vh$ , where  $A$ ,  $f$ , and  $\lambda$  are, respectively, the amplitude, frequency, and wavelength of the traveling

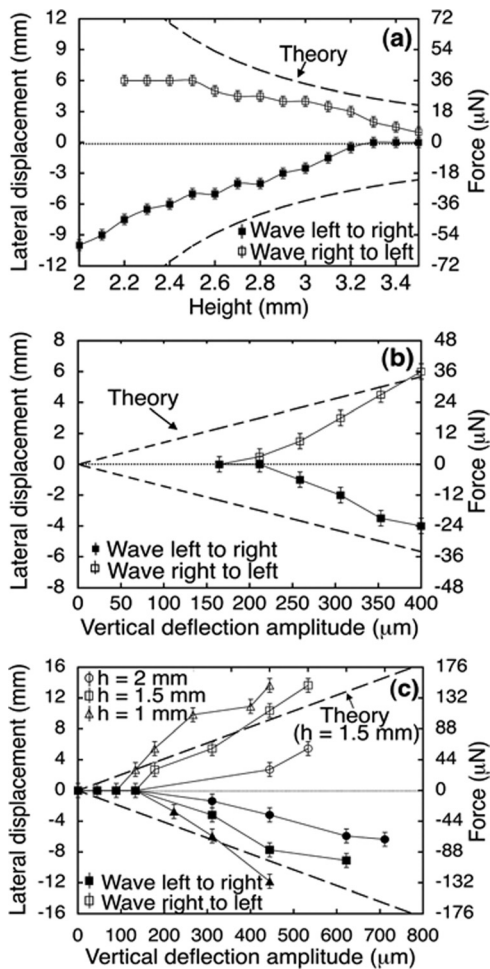


FIG. 4. Propulsive force measurements. All data shown is for traveling waves with at 100 Hz. (a) and (b) are from the pendulum arrangement, while (c) is from the “air-table” arrangement. Positive displacements correspond to motion of the sheet to the right. (a) The measured displacement, and calculated and predicted propulsive force, drops rapidly as the sheet is raised. Data shown are for waves at  $\sim 400 \mu\text{m}$  amplitude. (b) Above some threshold, the observed displacement, and hence the propulsive force, increases linearly with deflection amplitude. Data and theory are for the sheet  $\sim 2 \text{ mm}$  above the ground. (c) The displacement and propulsive force increase with amplitude and decrease with height above the ground. Note: error bars represent measurement precision.

wave (valid for  $A < h$ ).<sup>4</sup> This result follows since, when a sheet moves laterally close to a boundary, it pulls along approximately the entire volume of air under it (Fig. 5). By comparing with the drag force  $F_{drag}$ , we see that the theoretical propulsive force produced by the wave is

$$F_p \approx \frac{Af\lambda\mu_{air}WL}{h^2}. \quad (1)$$

The second (right) y-axis of Fig. 4(a) shows the propulsive force calculated from the displacement data, and the theory is then also plotted versus the suspension height. For simplicity, we assume equality in Eq. (1), which is reasonable based on the detailed simulation from Ref. 4. We observe qualitatively good agreement with this theory. The expected surface effect is quite strong, with the force decreasing rapidly as the sheet is raised. Figures 4(b) and 4(c) show the displacement and propulsive force (experimental and theoretical) versus wave amplitude for both the suspension and air table experi-

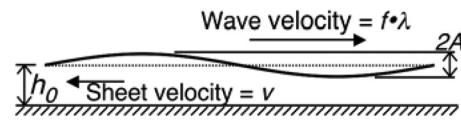


FIG. 5. Airflow balance schematic. In equilibrium, air pushed backwards by the wave ( $\sim Af\lambda$ ) must balance air pushed forward by the sheet ( $\sim v h_0$ ).

ments (for the air table, height is adjusted by varying the air pressure). Propulsive forces in excess of  $100 \mu\text{N}$  are created. Both arrangements give similar results, and qualitative agreement of magnitudes and trends are again observed. Theoretically, we expect a linear dependence of force on wave amplitude, but instead, we observe a linear increase only after some threshold, which may be due to the fact that the sheet is not perfectly flat.

As a further proof of the aerodynamic nature of the propulsive force, we measured the velocity of the air beneath the sheet by injecting smoke at one end of the sheet and measuring the time until it exits the other end (without a traveling wave, the smoke simply rises). With the sheet bending in a traveling wave, the smoke flows under the sheet at a speed of at least  $5 \text{ cm/s}$  (at conditions corresponding to the maximum displacement shown in Figure 4), in the same direction as the wave, as expected.

Some biological organisms use traveling wave-like deformations for propulsion in water.<sup>1,2</sup> Previous work has demonstrated propulsive forces from shape deformations on the microscopic scale by using magnetic fields to oscillate microscopic filaments of magnetic particles in a water-based salt solution,<sup>6</sup> resulting in swimming velocities of  $\sim 10 \mu\text{m/s}$ . More recently, propulsion has been induced by periodic contraction of a “muscular thin-film” in water,<sup>7</sup> although the exact shape was not clear. The velocities reported were still only  $\sim 200 \mu\text{m/s}$ , much smaller than the  $\sim 1 \text{ cm/s}$  velocities we have observed. Furthermore, traveling-wave induced propulsive forces are much smaller in air (for the same wave parameters), due to the lower viscosity, and this effect has not been previously reported.

In conclusion, traveling waves have been produced with amplitudes up to  $\sim 500 \mu\text{m}$ , and at 100 Hz, we have measured forces exceeding  $100 \mu\text{N}$  (resulting in velocities over  $1 \text{ cm/s}$ ) when the sheet is suspended  $\sim 1 \text{ mm}$  above the ground. The aerodynamic propulsive force that we have demonstrated is theoretically sufficient to achieve “flying” of the sheet, provided that it can be freed from its tethers (given the lift force predicted by Ref. 4 for our measured propulsive force). This work also demonstrates the advantages, in general, of using integrated sensors to control the dynamic shape of thin plastic sheets deformed by piezoelectric elements.

<sup>1</sup>G. I. Taylor, *Proc. R. Soc. London, Ser. A* **209**, 447 (1951).

<sup>2</sup>A. J. Reynolds, *J. Fluid Mech.* **23**(2), 241 (1965).

<sup>3</sup>G. I. Taylor, National Committee for Fluid Mechanics Films No. 21617 (1967).

<sup>4</sup>M. Argentina, J. Skotheim, and L. Mahadevan, *Phys. Rev. Lett.* **99**, 224503 (2007).

<sup>5</sup>K. P. Selverov and H. A. Stone, *Phys. Fluids* **13**, 1837 (2001).

<sup>6</sup>R. Dreyfus, J. Baudry, M. L. Roper, M. Fermigier, H. A. Stone, and J. Bibette, *Nature* **437**, 862 (2005).

<sup>7</sup>A. W. Feinberg, A. Feigel, S. S. Shevkopyas, S. Sheehy, G. M. Whitesides, and K. K. Parker, *Science* **317**, 1366 (2007).